10.1109/ULTSYM.2009.0356

An Improved Method for Tomographic Density Imaging Using a Multiple Frequency Inverse Scattering Approach

Roberto J. Lavarello and Michael L. Oelze
Bioacoustics Research Laboratory
Department of Electrical and Computer Engineering
University of Illinois at Urbana-Champaign
Urbana, IL 61801
Email: lavarell@illinois.edu

***Abstract*—Current inverse scattering methods for quantitative density imaging have limitations that keep them from practical experimental implementations. In this work an improved approach, termed the multiple frequency distorted Born iterative method (MF-DBIM) algorithm, was developed for imaging density variations. The MF-DBIM approach consists of inverting the wave equation by solving for a single functional that depends on both sound speed and density variations at multiple frequencies. Density information was isolated by using a linear combination of the reconstructed single-frequency profiles. The results were compared to reconstructions using methods currently available in the literature, i.e., the dual frequency DBIM (DF-DBIM) and T-matrix approaches. The performance of the MF-DBIM was assessed by reconstructing cylindrical targets of different radii, speed of sound and density contrasts. The MF-DBIM required the use of frequency hopping in order to converge to a proper solution. Useful density reconstructions, i.e., root mean square errors (RMSEs) less than 30%, were obtained even with 2% Gaussian noise in the simulated data and using frequency ranges spanning less than an order of magnitude. Therefore, the MF-DBIM approach largely outperformed both the DF-DBIM method (which has problems converging with noise even an order of magnitude smaller) and the T-matrix method (which requires a ka factor close to unity in order to achieve convergence). The MF-DBIM performance degraded severely when the angular coverage on reception was less than 180°. Although the MF-DBIM performance also degraded as the frequency jump magnitude increased, the RMSEs were not largely affected when the frequency jump was smaller than 5% of the maximum frequency used for the reconstructions.**

I. Introduction

Current acoustic tomography scanners [1]–[3] are capable of obtaining images of speed of sound and acoustic attenuation. Although there are many potential benefits of performing density imaging, to this date not a single acoustic tomography scanner is capable of obtaining such images. The most important reason is the lack of robust algorithms designed for this task that can be experimentally implemented. In particular, the DF-DBIM [4] and T-matrix [5] methods outlined in [6] require excessively high signal-to-noise ratios and large bandwidths, respectively. Therefore, it becomes necessary to develop improved techniques for density imaging if this modality is to be experimentally implemented.

One possibility for developing better density imaging techniques is to improve upon currently available algorithms. In particular, the DF-DBIM algorithm requires a relatively small bandwidth and therefore appears amenable to experimental implementation if the high sensitivity to noise can be overcome. The remainder of this work is devoted to the derivation and assessment of a variation of the DF-DBIM approach, termed here the multiple frequency DBIM (MF-DBIM) approach. Several aspects of the proposed algorithm have been explored, including the effects of density and speed of sound contrasts, sensitivity to noise, and the effects of algorithmic variables such as the bandwidth, the separation among frequencies used in the inversion, and the angular coverage on reception.

II. Methods

A. The Use of Multiple Frequency Information for Density Imaging

When using the distorted Born iterative method (DBIM) for tomographic imaging, the reconstructed object function $\mathcal{O}(\vec{r})$ depends on both density $\rho(\vec{r})$ and sound speed $c(\vec{r})$ as

$$\mathcal{O}(\vec{r}) = \left(\frac{\omega^2}{c^2(\vec{r})} - \frac{\omega^2}{c_0^2}\right) - \rho^{1/2}(\vec{r})\nabla^2\rho^{-1/2}(\vec{r}). \quad (1)$$

A minimum of two estimates of $\mathcal{O}(\vec{r})$ at two different frequencies are required in order to separate the speed of sound and density information, which corresponds to the DF-DBIM approach. However, if a set of reconstructions $\mathcal{O}_i = \mathcal{O}(\vec{r}, \omega_i)$ at frequencies ω_i, $i = 1, 2, ..., N_f$ are available, the least mean squares estimator

$$\mathcal{F}_\rho(\vec{r}) = \frac{\left(\sum_{i=1}^{N_f}\omega_i^2\right)\left(\sum_{i=1}^{N_f}\omega_i^2\mathcal{O}_i(\vec{r})\right) - \left(\sum_{i=1}^{N_f}\omega_i^4\right)\left(\sum_{i=1}^{N_f}\mathcal{O}_i(\vec{r})\right)}{N_f\sum_{i=1}^{N_f}\omega_i^4 - \left(\sum_{i=1}^{N_f}\omega_i^2\right)^2} \quad (2)$$

allows for the separation of speed of sound and density profiles. The use of multiple frequency information to improve upon the DF-DBIM approach was briefly explored by combining the profiles independently obtained at frequencies between f_{min} and f_0 in steps of Δf. The results when reconstructing cylinders with $\rho_r = 1/c_r$ and radius 2λ and 4λ using $\Delta f = 0.01 f_0$ are shown in Fig. 1.

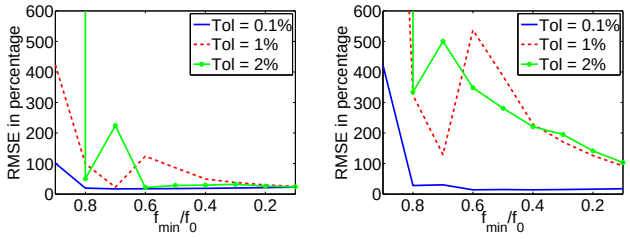

Fig. 1. RMSEs in density reconstructions using multiple frequency information. The error curves correspond to the reconstructions of circular cylinders with $\Delta\phi = 0.9\pi$, $\rho_r = 1/c_r$ and radius 2λ (left) and 4λ (right).

The use of multiple frequency information alone by using (2) to isolate the density term in (1) did not provide robust results. The error curves exhibit erratic behavior when the termination tolerance increases and reveal several frequencies at which excessively large errors occur. In particular, density reconstruction errors became more erratic when larger cylinders were imaged.

B. The Multiple Frequency DBIM (MF-DBIM) Approach

Given the ill-conditioning of the density imaging equation, the quality of the density reconstructions when using (2) is compromised by improper cancellation of the speed of sound components of the reconstructed $\mathcal{O}_i(\vec{r})$. This effect is exacerbated when large termination tolerance values are used, which reduces the correlation among the speed of sound components at different frequencies.

Here it is hypothesized that frequency hopping [7], i.e., the use of lower frequency estimates as initial guess for higher frequency reconstructions, may improve on the speed of sound term cancellation by providing a better initial guess than an all-zero vector. One important detail when using frequency hopping is the proper selection of the initial guess at higher frequencies. If the initial guess is too close to the true profile, no iterations will occur when processing the data at frequency ω_i for a given termination tolerance. On the other hand, if the initial guess is too far away from the true profile, correlation will be lost between $\mathcal{O}_{i-1}(\vec{r})$ and $\mathcal{O}_i(\vec{r})$. Therefore, the initial guess when processing the i-th frequency was chosen as

$$\mathcal{O}^{(0)}_{i,\text{MF-DBIM}}(\vec{r}) = (1 - 1.5t\%) \left(\frac{\omega_{i-1}}{\omega_i}\right)^2 \mathcal{O}_{i-1}(\vec{r}), \quad (3)$$

where $t\%$ is the termination tolerance. The contraction factor of $(1 - 1.5t\%)$ was used to guarantee that the resulting scattered field discrepancy is larger than $t\%$. For the lowest frequency f_{min} used the initial guess was chosen as an all-zero vector. The use of (2) with frequency hopping and (3) as initial guess selection rule has been termed here the multiple frequency DBIM (MF-DBIM) approach. For the rest of this work, this hypothesis will be evaluated by assessing the ability of this approach to reconstruct circular cylinders as in [6].

III. Results

A. Noise robustness

A preliminary evaluation of the MF-DBIM approach with $\Delta f = 0.01 f_0$ was obtained through reconstructions of cylindrical imaging targets with excess phase $\Delta\phi = 0.9\pi$, $\rho_r = 1/c_r$, and radii 2λ and 4λ. A termination tolerance of 2% was used, both with noiseless data and noisy data with 2% Gaussian noise. The mean and standard deviation of the reconstruction RMSEs in the presence of noise were calculated using ten different noise realizations. The results are shown in Fig. 2. For comparison, the error curves when using DF-DBIM with noiseless data and 0.1% and 2% termination tolerances are also presented.

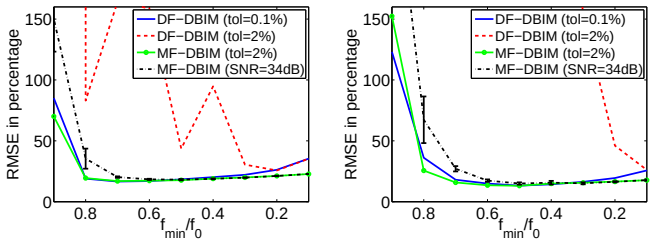

Fig. 2. RMSEs in density reconstructions of cylinders with $\rho_r = 1/c_r$, $\Delta\phi = 0.9\pi$ and radius 2λ (left) and 4λ (right). The RMSEs when using DF-DBIM at 0.1% (blue) and 2% (red) tolerance, and MF-DBIM at 2% tolerance with noiseless (green) and noisy (black) data are shown.

When reconstructing density from noiseless data and 2% termination tolerance, MF-DBIM provided comparable reconstructions to the ones obtained with DF-DBIM and 0.1% tolerance. In fact, MF-DBIM slightly but consistently outperformed DF-DBIM at low frequencies. At 2% termination tolerance, the reconstructions using DF-DBIM exhibited significantly larger errors when compared to those obtained with the MF-DBIM counterpart. The reconstructions using noisy data degraded when compared to those using noiseless data for high values of f_{min}, but were virtually unchanged when moderate to large bandwidths were used. Therefore, the MF-DBIM method appears to significantly extend the SNR limitation of the DF-DBIM approach.

B. Effects of speed of sound and density contrasts

The dependence of the performance of the MF-DBIM approach on speed of sound and density contrasts was evaluated by reconstructing circular cylinders of radii λ, 2λ, and 4λ. The effects of speed of sound contrast were studied by fixing $\rho_r = 1/c_r$ and changing the speed of sound to obtain $\Delta\phi$ values of 0.9π, -0.9π, 0.45π, and -0.45π, where $\Delta\phi$ is the maximum excess phase the incident wave accumulates when propagating through the cylinder. The effects of density contrast were studied using cylinders with fixed $\Delta\phi = 0.9\pi$ and relative density ρ_r values of $1/c_r$, $1/c_r^2$, $1/c_r^4$, and c_r,

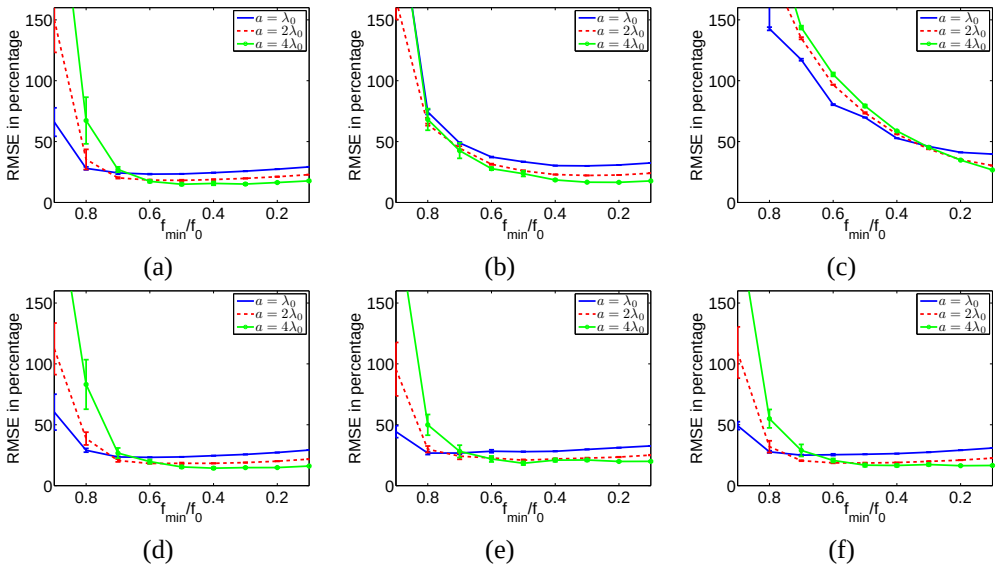

Fig. 3. RMSEs in density reconstructions of circular cylinders using the MF-DBIM approach. The corresponding properties of the cylinders are (a) $\rho_r = 1/c_r$, $\Delta\phi = 0.9\pi$, (b) $\rho_r = 1/c_r^2$, $\Delta\phi = 0.9\pi$, (c) $\rho_r = 1/c_r^4$, $\Delta\phi = 0.9\pi$, (d) $\rho_r = 1/c_r$, $\Delta\phi = -0.9\pi$, (e) $\rho_r = 1/c_r$, $\Delta\phi = 0.45\pi$, and (f) $\rho_r = 1/c_r$, $\Delta\phi = -0.45\pi$.

where c_r is the relative speed of sound. For all simulations, the frequency hop Δf was set to $0.01 f_0$ and the results were obtained using a termination tolerance of 2% and noisy data with ten different noise realizations at an SNR of 34 dB. The results are shown in Fig. 3.

The speed of sound contrast was not observed to play an important role in the convergence of the analyzed cases. Density contrast was found to have more of an effect on the behavior of the error curves. These trends are similar to the ones corresponding to the DF-DBIM approach [6], and indicate that the performance of the MF-DBIM approach is imaging target dependent. However, the results presented here suggest that MF-DBIM is capable of extending the SNR limitations of DF-DBIM while using significantly smaller bandwidths than the ones required by the T-matrix approach [6]. Therefore, the MF-DBIM approach appears to outperform currently available methods for tomographic density imaging in terms of experimental implementation feasibility.

For all cases, the standard deviation of the reconstruction RMSEs decreased with decreasing f_{min} values due to at least two factors. First, more frequencies are used when a lower f_{min} value is chosen and therefore some reduction in the variations of $\mathcal{F}_\rho(\vec{r})$ follow. Second, noise amplification when using (2) to isolate $\mathcal{F}_\rho(\vec{r})$ is less severe when using a lower f_{min} value. This improvement in precision is gained at the expense of spatial resolution, but the presented results suggest that the MF-DBIM approach alleviates the loss of spatial resolution when compared to the simpler DF-DBIM case.

C. Effects of the frequency separation Δf

The effects of Δf in the reconstruction errors when imaging circular cylinders with $\Delta\phi = 0.9\pi$ and ρ_r values of $1/c_r$ and $1/c_r^2$ are shown in Fig. 4. The RMSEs increased with increasing Δf, which is expected due to the reduced number of measurements and loss of correlation among different $\mathcal{O}(\vec{r})$ estimates. For the studied cases, the performance did not degrade significantly even when $\Delta f = 0.05 f_0$ for $f_{min} \leq 0.5 f_0$.

D. Effects of the angular coverage on reception $\Delta\theta$

The effects of changing the angular coverage on reception $\Delta\theta$ were also analyzed using the same simulation set of Section III-C, where $\Delta\theta$ is defined as the range of scattering angles centered around the forward scattering direction at which the scattered field is measured for each transmitter position. For all simulations, the overdetermination factor was kept equal to 2 by increasing the sampling density and the number of transmitters as $\Delta\theta$ decreased. Reception angular coverages of $360°$, $270°$, $180°$, and $90°$ were used. The corresponding reconstruction errors are shown in Fig. 5.

The reconstruction errors increased severely as $\Delta\theta$ was reduced below $90°$. This is consistent with (1), which predicts that density effects on $\mathcal{O}(\vec{r})$ are high-pass filtered and therefore concentrated away from forward scattering directions. It is interesting to notice that in the case of $\rho_r = 1/c_r^2$ the reconstruction errors actually improved at reduced $\Delta\theta$ values, as long as $\Delta\theta > 180°$. Therefore, the smoothing of the reconstructed profiles seems to have a self-regularizing effect in the reconstructions. This effect still allows the production of useful images as long as the angular coverage is kept above a certain threshold.

IV. Conclusions

In summary, the MF-DBIM approach outperformed currently available density imaging methods and required SNR levels and bandwidth ranges that are obtainable using current ultrasonic tomography scanner technology. The performance of MF-DBIM, just like the one for the DF-DBIM and T-matrix

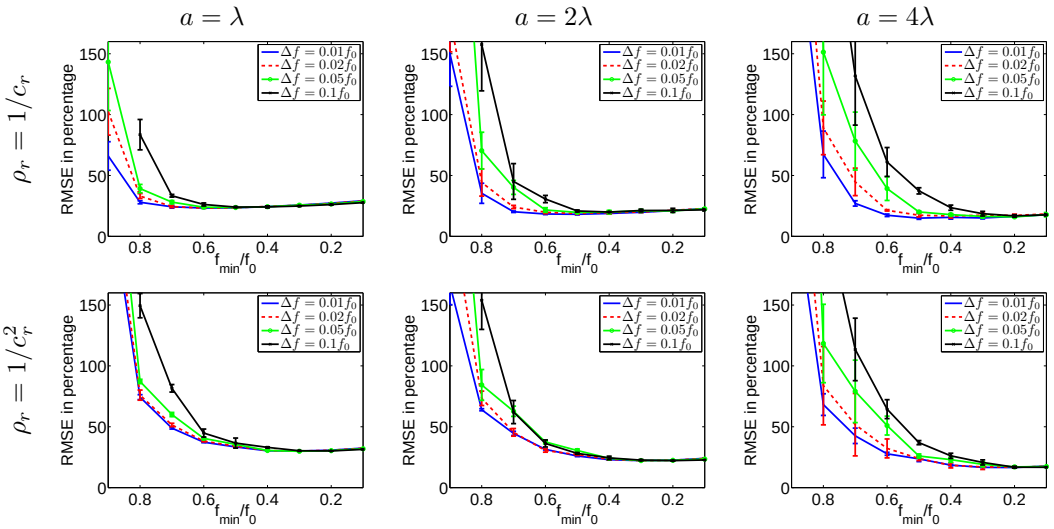

Fig. 4. Effect of Δf in the RMSEs of density reconstructions of λ (first column), 2λ (second column), and 4λ (third column) radius cylinders with $\rho_r = 1/c_r$ (top) and $\rho_r = 1/c_r^2$ (bottom) using MF-DBIM. The SNR was set to 34 dB for all cases.

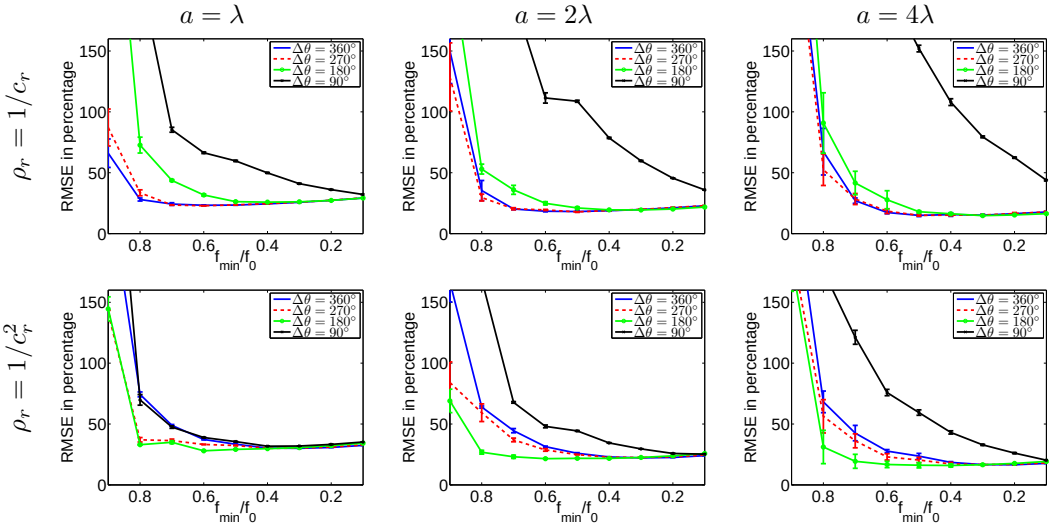

Fig. 5. Effect of $\Delta\theta$ in the RMSEs of density reconstructions of λ (first column), 2λ (second column), and 4λ (third colum) radius cylinders with $\rho_r = 1/c_r$ (top) and $\rho_r = 1/c_r^2$ (bottom) using MF-DBIM. The SNR was set to 34 dB for all cases.

approaches, was found to be dependent on acoustic properties of the imaging target. Although this technique is more amenable for experimental implementation than previously available methods, the effects of non-random measurement errors (i.e., instrument calibration errors) should be taken into account for a robust implementation of the technique.

REFERENCES

[1] J.-W. Jeong, T.-S. Kim, D. C. Shin, S. Do, M. Singh, and V. Z. Marmarelis, "Soft tissue differentiation using multiband signatures of high resolution ultrasonic transmission tomography," *IEEE Transactions on Medical Imaging*, vol. 24, no. 3, pp. 399–408, March 2005.

[2] S. A. Johnson, T. Abbott, R. Bell, M. Berggren, D. Borup, D. Robinson, J. Wiskin, S. Olsen, and B. Hanover, "Noninvasive breast tissue characterization using ultrasound speed and attenuation," in *Acoustical Imaging*, vol. 28, 2007, pp. 147–154.

[3] C. Li, N. Duric, and L. Huang, "Breast imaging using transmission ultrasound: Reconstructing tissue parameters of sound speed and attenuation," in *International Conference on BioMedical Engineering and Informatics*, vol. 2, 2008, pp. 708–712.

[4] M. J. Berggren, S. A. Johnson, B. L. Carruth, W. W. Kim, F. Stenger, and P. K. Kuhn, "Ultrasound inverse scattering solutions from transmission and/or reflection data," in *Proceedings of the SPIE*, vol. 671, 1986, pp. 114–121.

[5] J. Lin and W. Chew, "Ultrasonic imaging by local shape function method with CGFFT," *IEEE Transactions on Ultrasonics, Ferroelectrics, and Frequency Control*, vol. 43, no. 5, pp. 956–969, September 1996.

[6] R. J. Lavarello and M. L. Oelze, "Density imaging using inverse scattering," *Journal of the Acoustical Society of America*, vol. 125, no. 2, pp. 793–802, February 2009.

[7] W. C. Chew and J. H. Lin, "A frequency-hopping approach for microwave imaging of large inhomogeneous bodies," *IEEE Microwave and Guided Wave Letters*, vol. 5, no. 12, pp. 440–441, December 1995.